2. Neutron Diffraction in Solid State Physics

By C. G. Shull, Cambridge, Mass., USA

1. Neutron scattering characteristics

During recent years, neutron diffraction techniques have advanced to the stage where they now can be applied to many of the problems which are ordinarily studied with x-rays and electrons. This has been possible of course because of the availability of intense, slow neutron beams from reactors or piles and much of the progress has resulted because such reactors have become accessible to many research groups at different locations. Even now, there is very active consideration and planning for research reactors in Germany and active construction work should be started in the very near future.

Sufficient progress in the field of neutron diffraction has been made that general fields of application of the technique are now outlined. The present report will summarize these areas of application in very brief form along with a general introduction to the technique itself. Fairly complete reviews of the field are available [1] in the literature and additional details may be found in these and in the research publications.

2. Neutron properties

Associated with a moving particle is its *de Broglie* wavelength and it is fortunate that the slow neutrons which emanate from a reactor or pile are of such velocities that their wave lengths are of the order of 1 Å. Fig. 1 shows a typical wavelength distribution for the ons from a reactor and it is seen that the spectrum is peaked at a wavelength of 1 Å. Unfortunately the distribution in wavelengths is too broad for the usual diffraction techniques and it is necessary to select a monochromatic section from the distribution with consequent loss of intensity. In practice this is done by *Bragg*-reflecting the neutron beam from a single crystal, usually of metallic type, lead or copper.

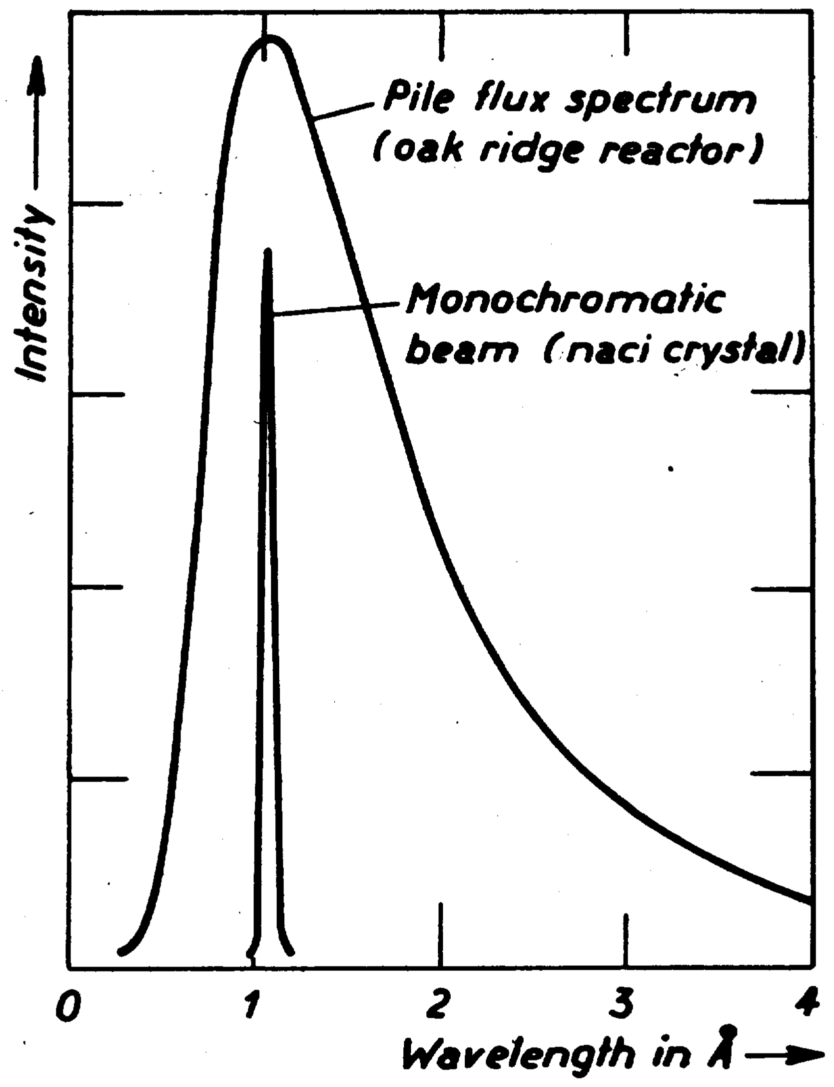

Fig. 1. Neutron spectrum from a typical reactor

Neutron scattering by an atom is usually through the nuclear force interaction with the nucleus and it has been established that the short range interaction with the electrons is very small and generally unobservable. Thus the neutron scattering amplitudes will change from one atom to another depending upon the characteristics of the nuclear force field and it is known from experimental data that wide variations exist in this. Fig. 2 shows the variation of the coherent neutron scattering amplitudes with increasing atomic mass and for comparison, some x-ray scattering amplitudes are also shown. It is seen that the regularity which characterizes the x-ray amplitudes is lost to a large extent in the neutron case. Moreover the neutron amplitudes are frequently found to differ among the various isotopes of a given element, and even to change sign, whereas this would not be the case for x-rays. This suggests one very important field of application for the neutron technique to those problems wherein the relative neutron amplitudes are more favorable to solution of the crystallographic structure than are the x-ray amplitudes.

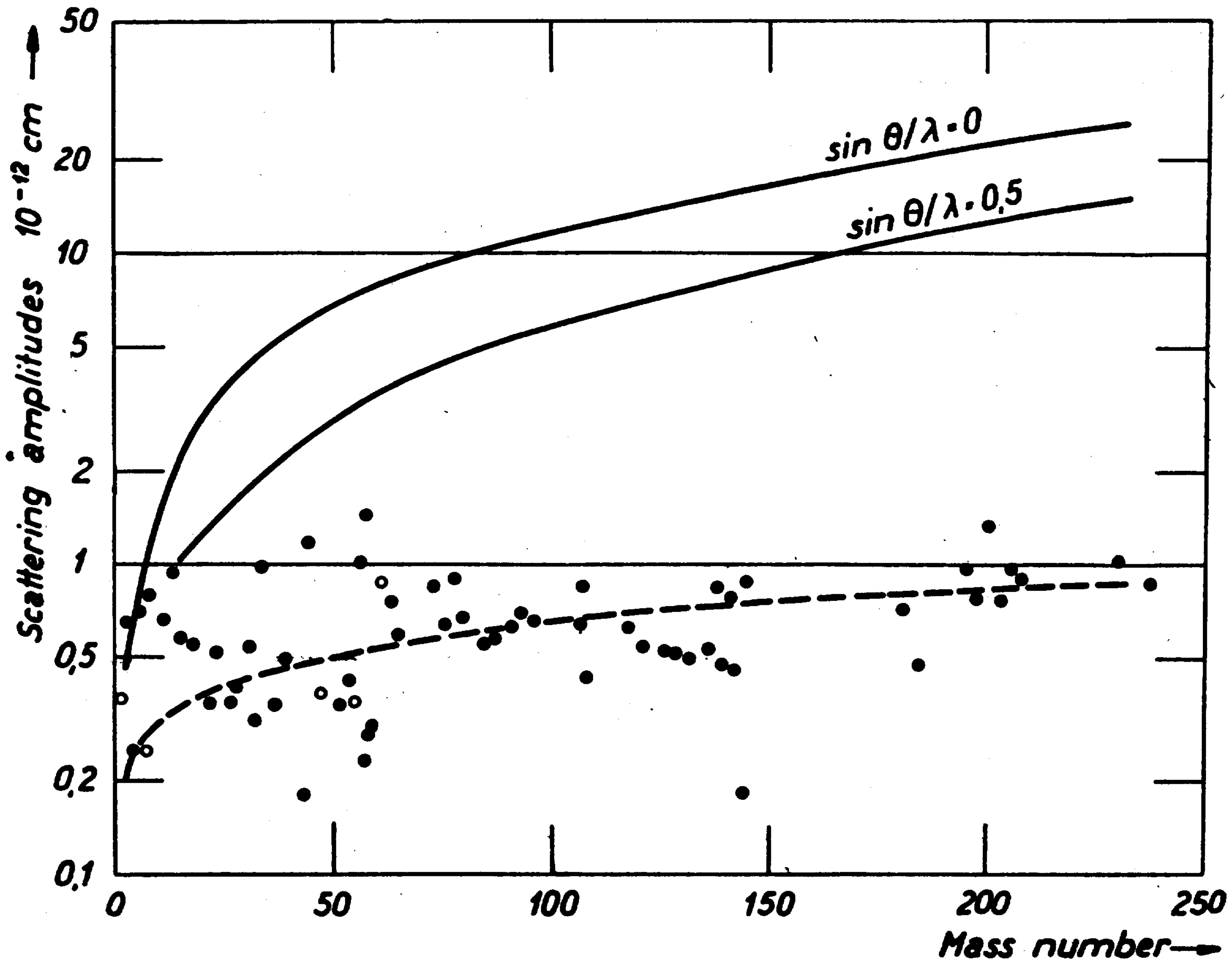

Fig. 2. Variation of coherent scattering amplitudes among the elements. The solid lines are for x-radiation and the points are for neutrons

Associated with the marked difference in scattering amplitudes is an even greater difference in the absorptive properties of atoms for the radiation. Fig. 3 shows the variation of the mass absorption coefficient again with atomic mass for neutrons and for x-radiation and it is seen that the former values are three or four orders of magnitude smaller than are the latter. This has the very practical consequence that specimens for neutron scattering study can be made quite thick of the order of one centimeter for maximum scattering.

Since neutrons are scattered by the nuclei and not in general by the electrons, the scattering is isotropic and independent of scattering angle because the

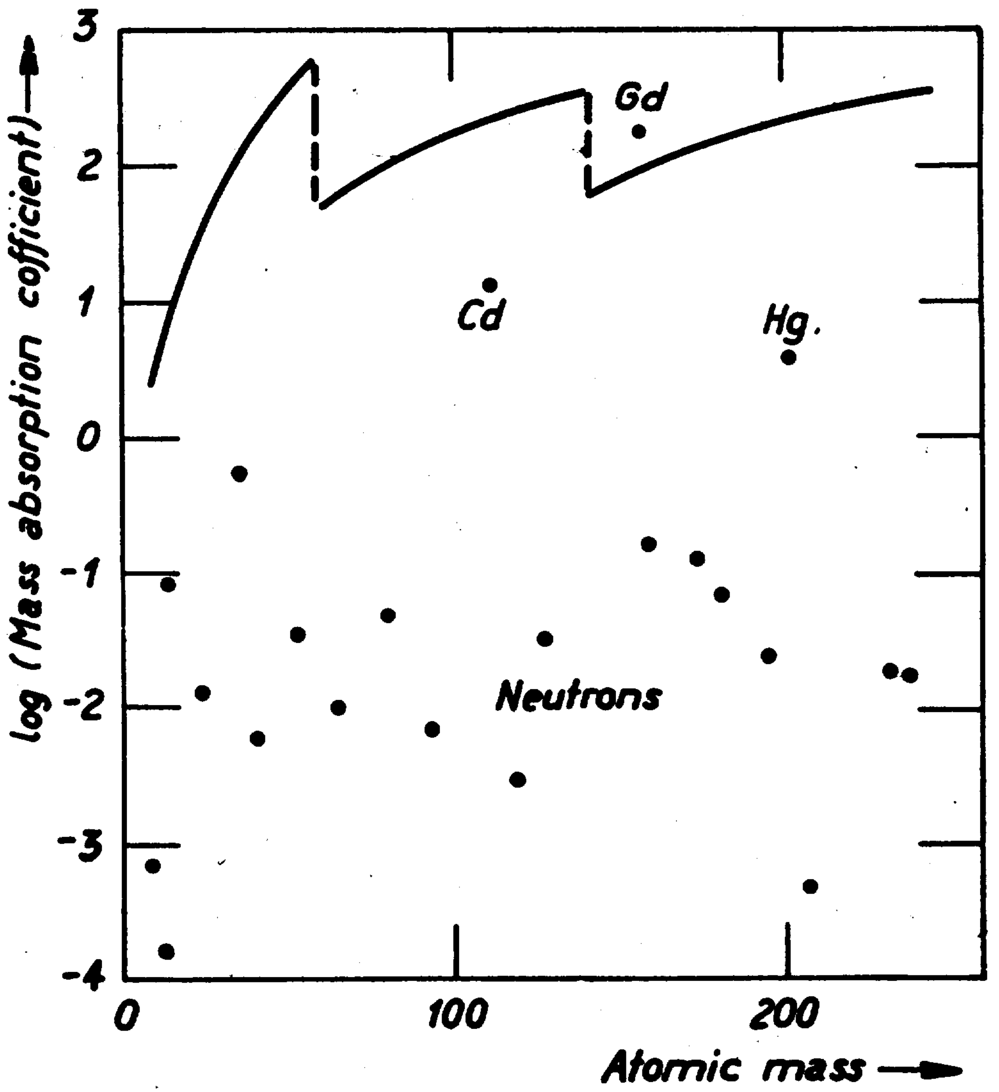

Fig. 3. Variation of mass adsorption coefficient for x-radiation and for neutrons

nuclear size (10^{-12} cm) is so very much smaller than the neutron wavelength (10^{-8} cm). Thus the atomic form factors which characterize x-ray scattering are lacking for the neutron case as is shown in Fig. 4.

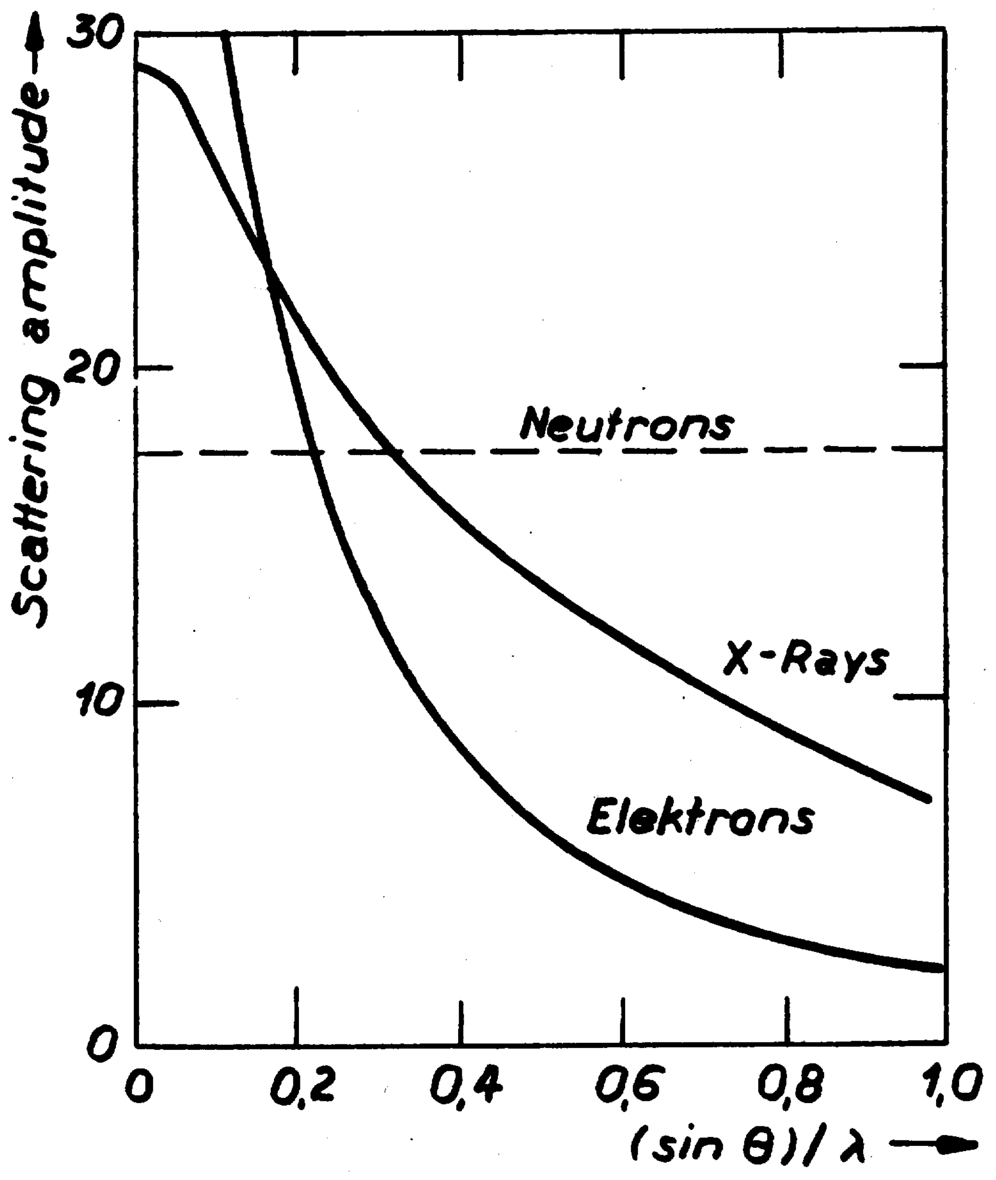

Fig. 4. Atomic form factors for various radiations

In addition to the nuclear force field scattering, neutrons can be scattered by atoms which possess an atomic magnetic moment. This magnetic dipole-dipole interaction can be calculated and is quite comparable in some cases to the nuclear interaction. Thus the magnetic scattering of neutrons can be used to determine details of the magnetic structure to a degree not possible by other techniques.

3. Neutron diffraction techniques

Fig. 5 shows a schematic diagram of a typical diffraction spectrometer along with an indication of the neutron intensities which are available at different parts of the spectrometer. A beam of neutrons is taken out through a collimating tube in the reactor shield and this is monochromatized by *Bragg* reflection from a large single crystal. Frequently this monochromatic beam is monitored by passage through a small neutron counter before it is scattered by the specimen located on a spectrometer table. The scattered radiation is finally detected with a gas proportional counter containing BF_3 with the enriched B^{10} isotope. Copious shielding of lead and borated paraffin is required around the monochromating crystal in order to absorb all of the unwanted γ-rays and fast neutrons which emanate from the reactor. Also it is customary to enclose the detecting counter in a smaller neutron shield to lower its background response. Some development work toward the use of scintillating crystals as detectors has been carried out but this has not reached the stage of practical usefulness as yet.

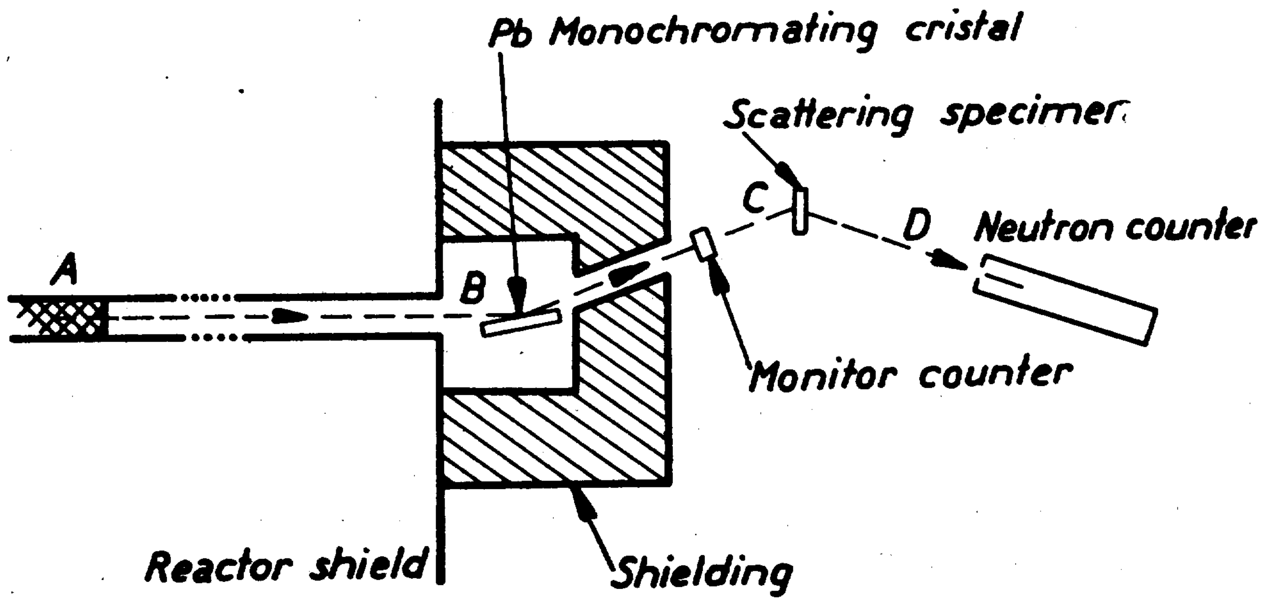

Fig. 5. Schematic diagram of neutron diffraction spectrometer. Neutron current densities of 10^7 per cm^2 sec (at B), 10^5 per cm^2 sec (at C) and 10 per cm^2 sec (at D) are obtained

Both polycrystalline and single crystal specimens have been studied. The area of the neutron beam and hence the size of the scattering specimen may be quite large for the powder diffraction case amounting to perhaps 25 cm^2 with a specimen thickness about 1 cm. In order to maintain suitable angular resolution with such a large beam, sets of Soller slits are frequently used. These are positioned in the monochromatic beam incident on the specimen and also in front of the detecting counter. Suitable intensity is obtained in the single crystal type of investigation with very much smaller samples ranging from 1 to 100 mm^3. Fig. 6 shows a photograph of a spectrometer recently installed at Brookhaven National Laboratory by *Drs. Corliss* and *Hastings*. This instru-

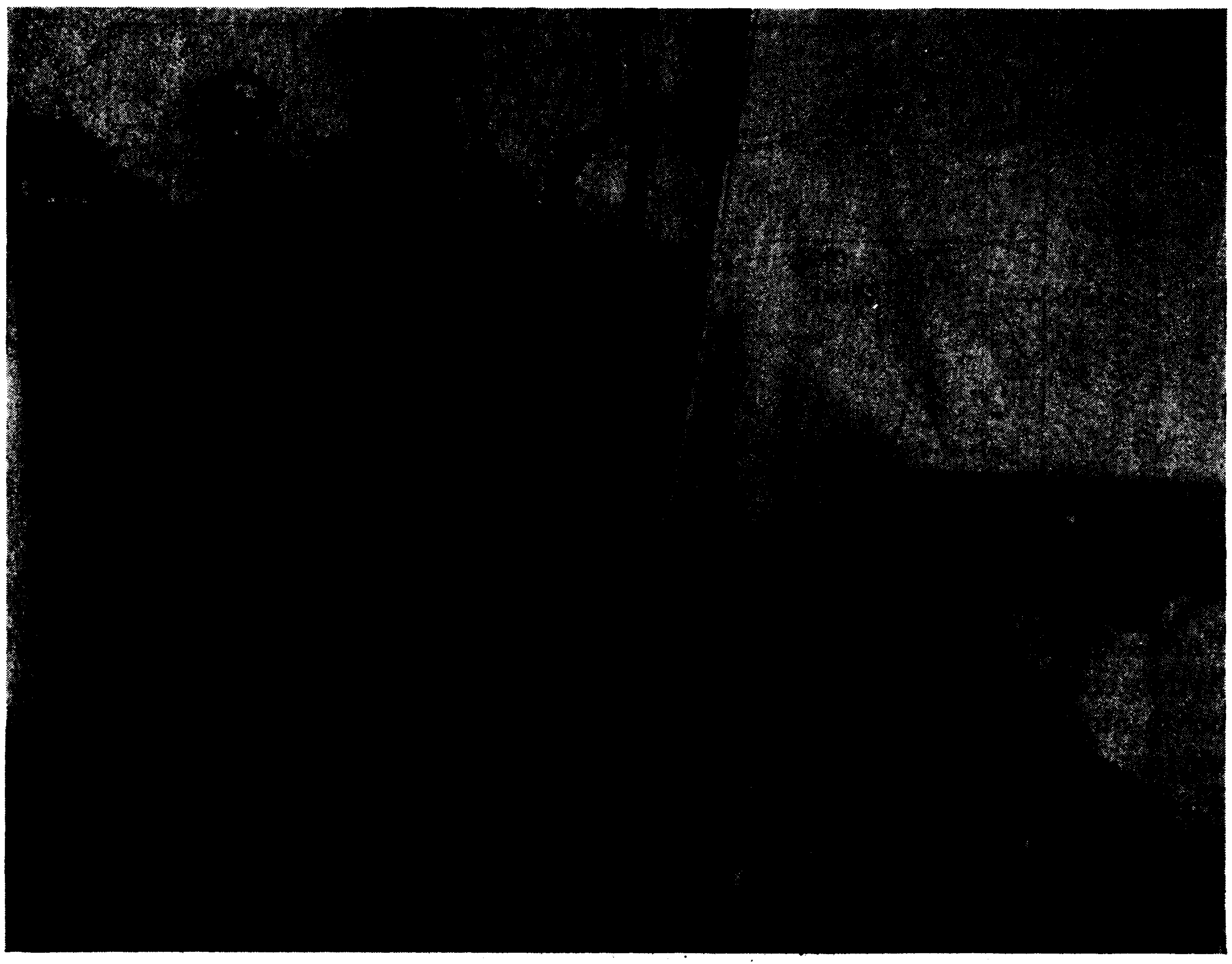

Fig. 6. Photograph of single crystal spectrometer (courtesy of Drs. *Corliss* and *Hastings*)

ment is primarily for single crystal investigation and since the neutron beam area is not too large (3 cm by 1 cm) the general size of the instrument is smaller than that used in powder diffraction work.

One very important feature of the neutron diffraction method is the ease with which the scattered intensities can be placed on an absolute scale. Since the specimen volumes can be measured easily and accurate monitoring of the primary beam intensity can be accomplished, the scattered intensities can be obtained on an absolute scale by suitable intercomparison with specimens of known scattering cross section. This has been performed in some cases to an accuracy of one half of one percent. The availability of absolute intensities, in addition to the normally obtained relative intensities, is of great usefulness in structure determinations.

4. Applications of the technique

Crystallographic investigations. The present report will summarize in very brief form a few of the problems which have been studied in two general areas of applications, namely crystallographic investigations and magnetic structure problems. In crystallographic studies the technique has its greatest value in cases where the neutron scattering amplitudes are more favorable than the equivalent x-ray or electron amplitudes for successful solution of the problem.

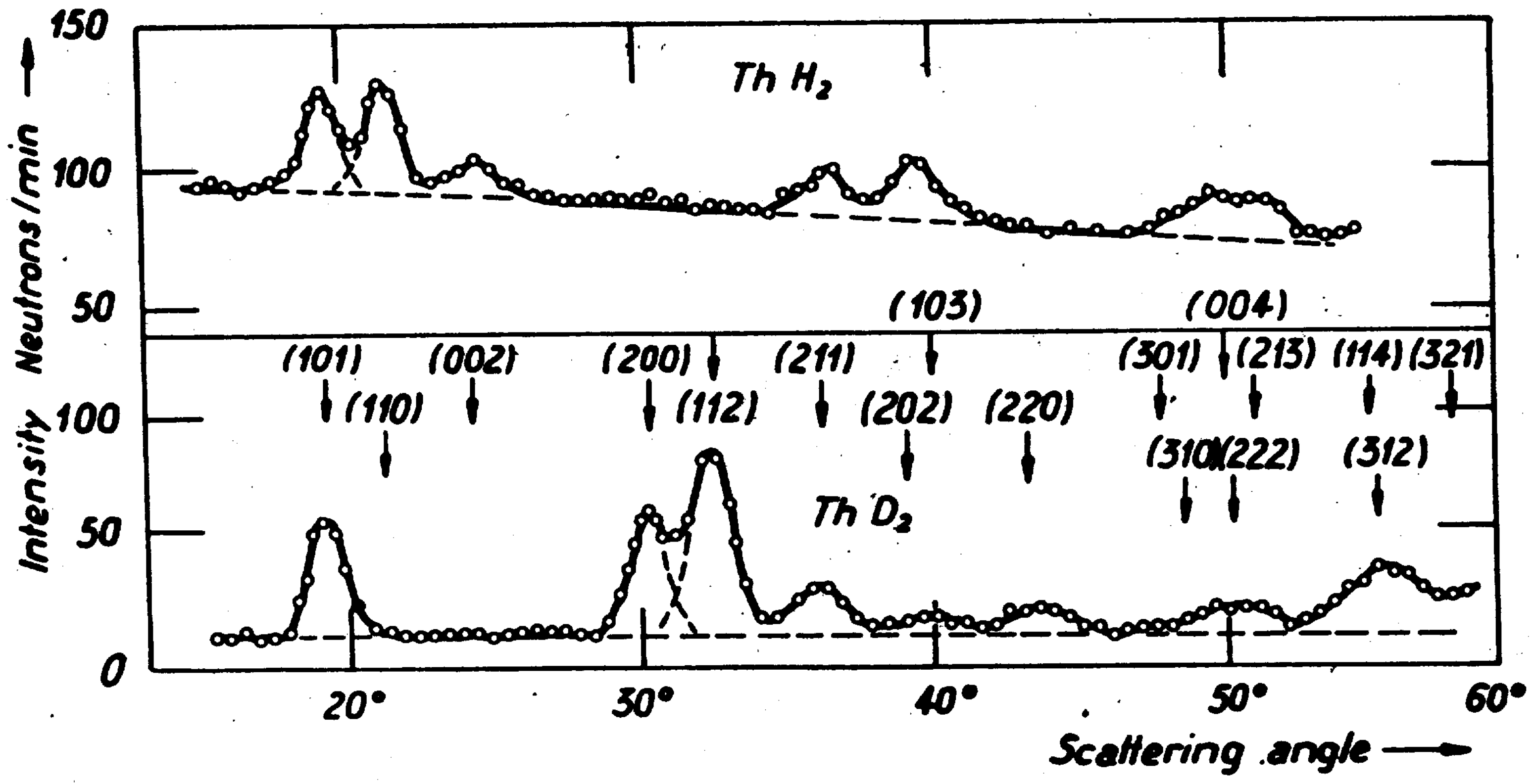

Fig. 7. Powder diffraction patterns of Th H_2 and Th D_2

Foremost in this classification are those problems dealing with the location of hydrogen atoms in crystal structures. With x-radiation the study of hydrogen-containing crystals is very difficult if not impossible because of the very small scattering power of a hydrogen atom relative to all of the other heavier atoms. This is not the case with neutron radiation and hence the diffractive effects produced by the hydrogen atoms in a crystal are quite pronounced and they can be positioned in the lattice with accuracy.

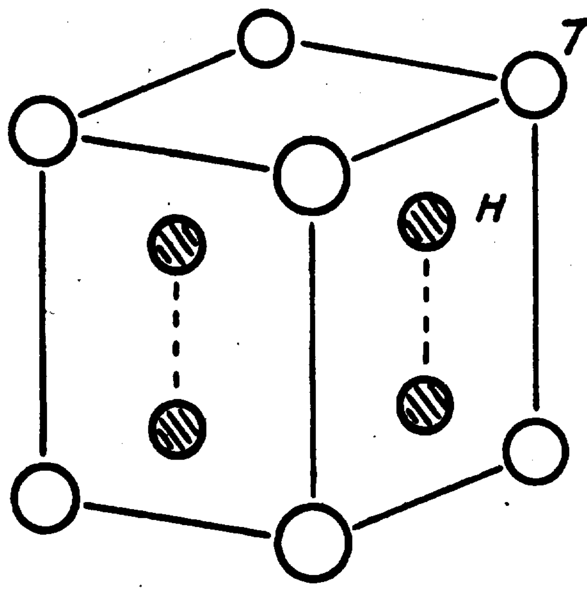

Fig. 8. Structure of Th H_2

As a typical example of a hydrogen-containing structure which has been studied by the *Debye-Scherrer* technique, we can look at the case of ThH_2. This represents an extreme case wherein very heavy atoms are combined with very light ones and Fig. 7 shows patterns [2] obtained for both ThH_2 and ThD_2. As is noticed in this figure, the two patterns differ greatly and this is because the two hydrogen isotopes differ considerably in the value of their scattering amplitudes, these being —0.378 and $+0.65 \cdot 10^{-12}$ cm. From these patterns it was easy to establish the structure as being body-centered tetragonal for the thorium ions with the hydrogen atoms located in the side faces as illustrated in Fig. 8. The examination of the patterns with both hydrogen isotopes serves as a very useful check on the validity of the structure.

Another very interesting hydrogen structure is that of ice and this has been studied in both the poly-crystalline and single crystal forms. Fig. 9 shows a typical *Fourier* projection of the neutron scattering density for D_2O ice as obtained recently by *Levy* and *Peterson*. The item of most interest here is the positioning of the hydrogen atom along the O—H—O bond linkage. Two equilibrium positions are suggested by the projection so that effectively a half hydrogen atom resides at each site. This supports the disordered structure model first proposed by *Pauling* some years ago.

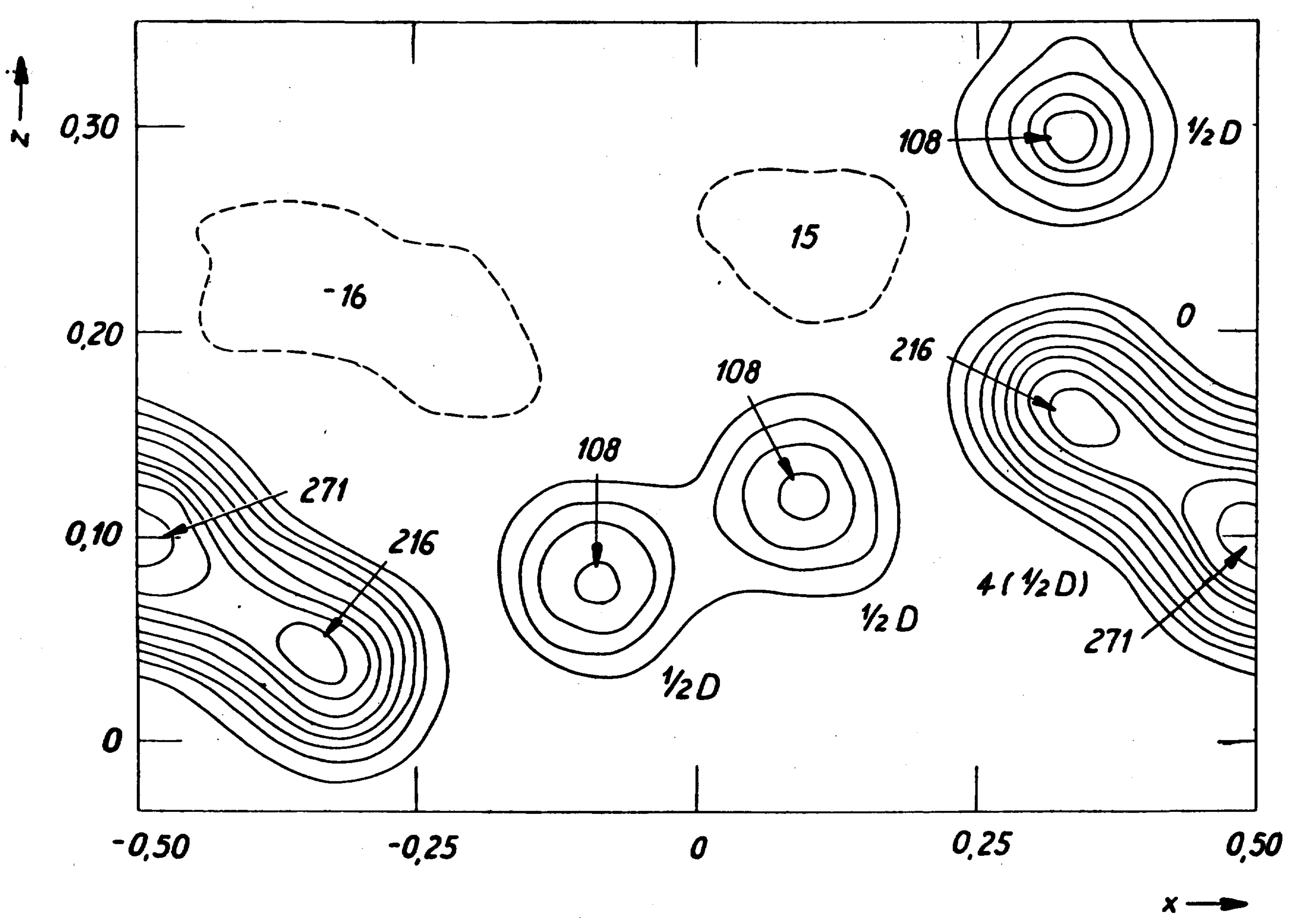

Fig. 9. Fourier projection of neutron scattering density for D_2O ice (from *Levy* and *Peterson*)

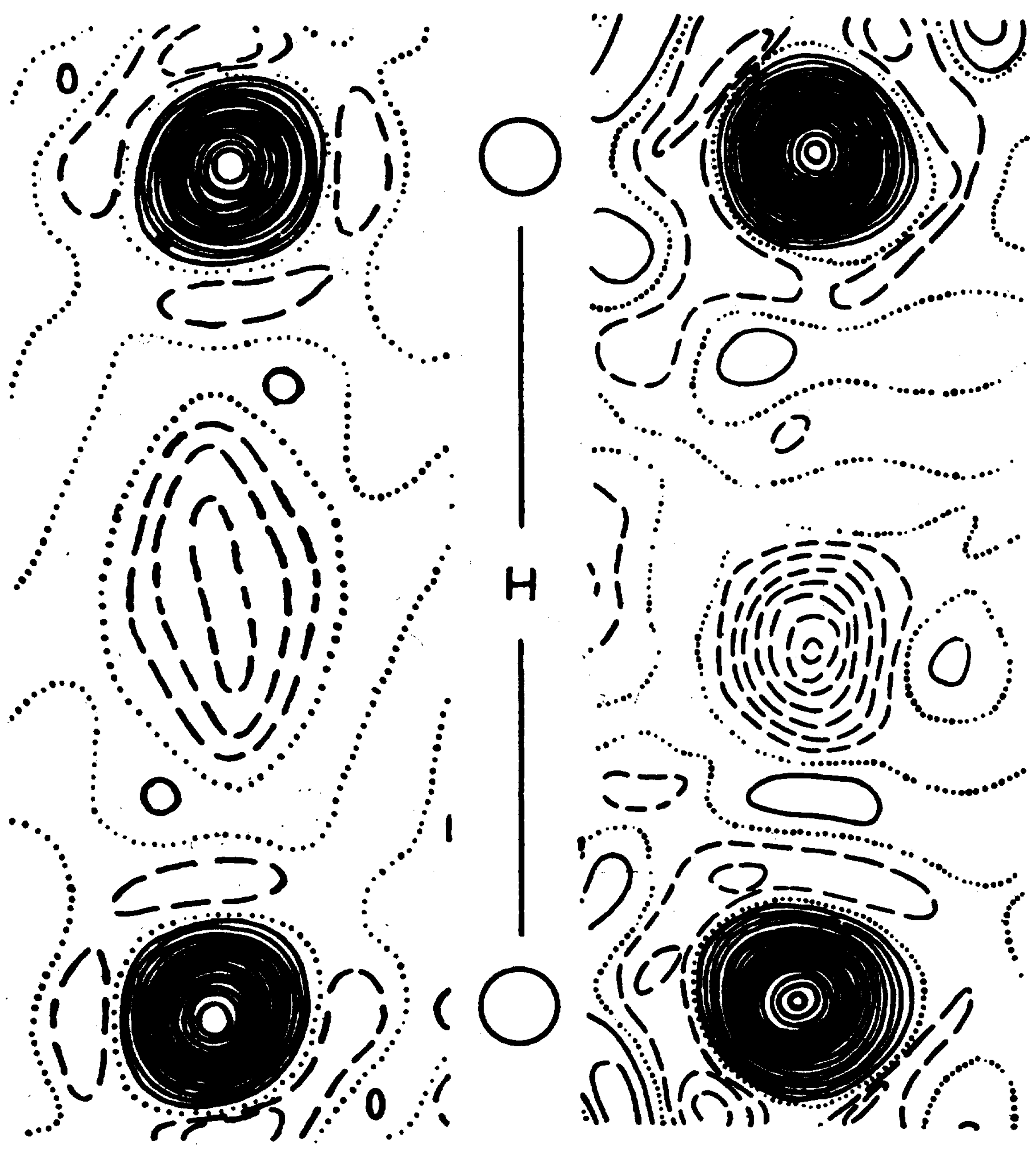

Fig. 10. Fourier projection of neutron scattering density for KH_2PO_4 above the ferroelectric Curie temperature (left side) and below T_C (right side). (from *Bacon* and *Pease*)

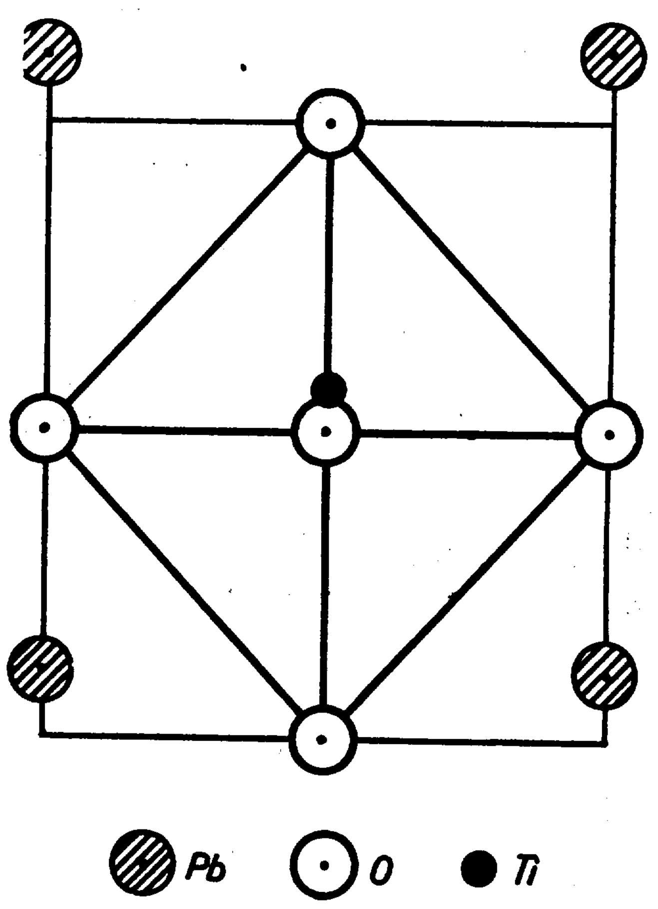

Fig. 11. Ferroelectric displacements in $PbTiO_3$ (from *Shirane, Pepinsky* and *Frazer*)

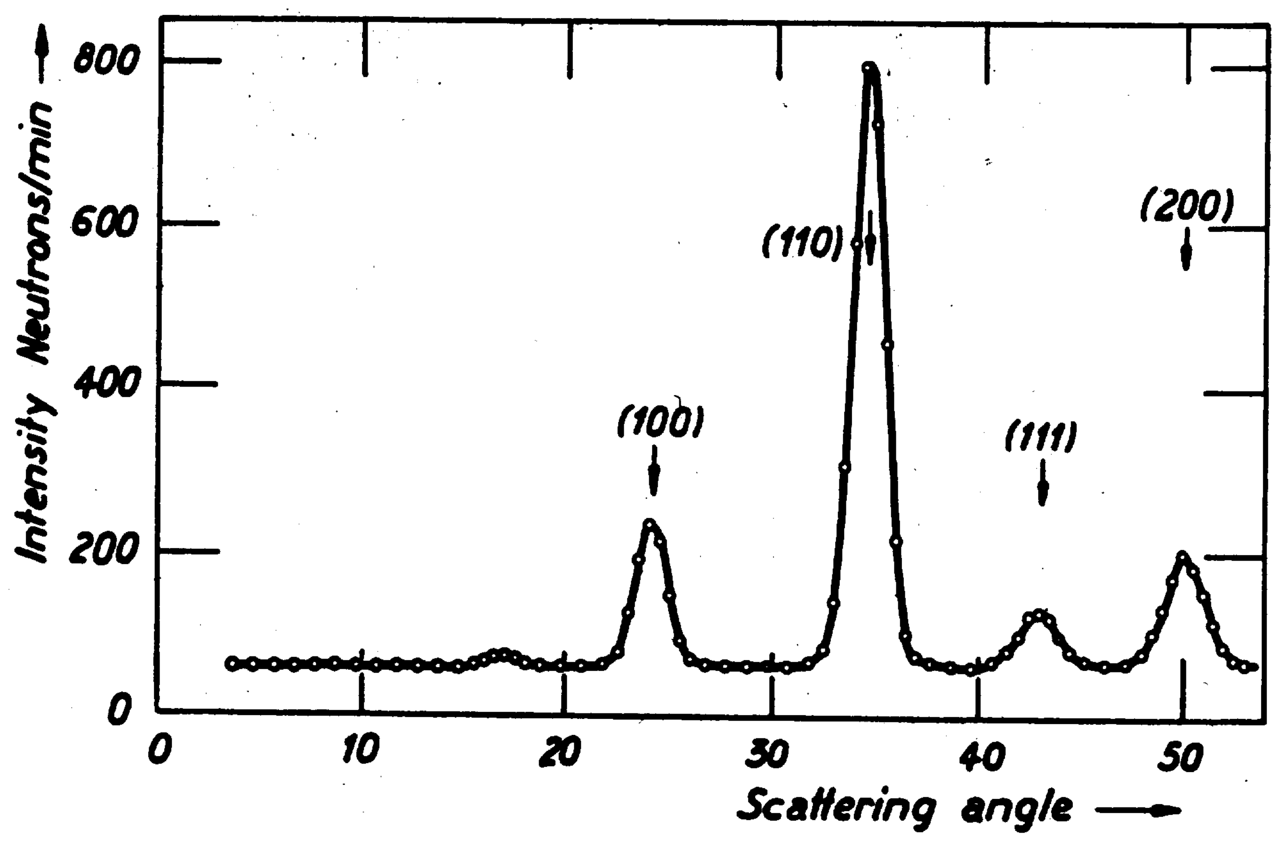

Fig. 12. Superstructure appearance in ordered FeCo

The third hydrogen structure to be illustrated is that for KH_2PO_4 which becomes ferroelectric at low temperatures. According to an early interpretation given by *Slater,* the onset of ferroelectricity was considered to result from a repositioning of the hydrogen atom along the O—H—O linkage. This structure has been studied by several groups, *Levy* and *Peterson, Pepinsky* and *Frazer,* and *Bacon* and *Pease* and Fig. 10 shows *Fourier* projections obtained by the latter group [3] at two temperatures above and below the ferroelectric Curie temperature of about 120 °K. It is seen that the hydrogen atom is positioned symmetrically between two oxygen atoms at the higher temperature whereas it is located at an off-center position in the ferroelectric state. This is of great significance in the understanding of the ion distribution responsible for the ferroelectricity.

Fig. 11 shows the ion distribution obtained by Shirane, Pepinsky and Frazer [4] in ferroelectric $PbTiO_3$ which again illustrates interesting ferroelectric displacements. The neutron scattering data serve as a very useful supplement to the x-ray data in establishing the relative displacements of the Pb and Ti ions with respect to the oxygens ions.

The neutron technique has been very useful in the study of ordering effects in alloys of transition elements and this is illustrated in the pattern of Fig. 12. The superstructure lines (100) and (111) are shown here for body centered cubic FeCo and these are of considerable intensity because the neutron scattering amplitudes for Fe and Co are favorably different. A number of studies have been performed on the sigma-phase and related ones.

5. Magnetic structure investigations

Probably the most unique application of the neutron diffraction technique is in the determination of magnetic structures. The neutron by virtue of its intrinsic magnetic moment can interact with any localized atomic magnetic moments which may be present in the scattering substance and this interaction manifests itself in the diffraction pattern. For paramagnetic substances in which the atomic magnetic moments are directed at random, the scattering will appear as incoherent or diffuse scattering with a characteristic form factor decline of intensity with increasing scattering angle. On the other hand, ferromagnetic and antiferromagnetic substances possess ordered magnetic moments

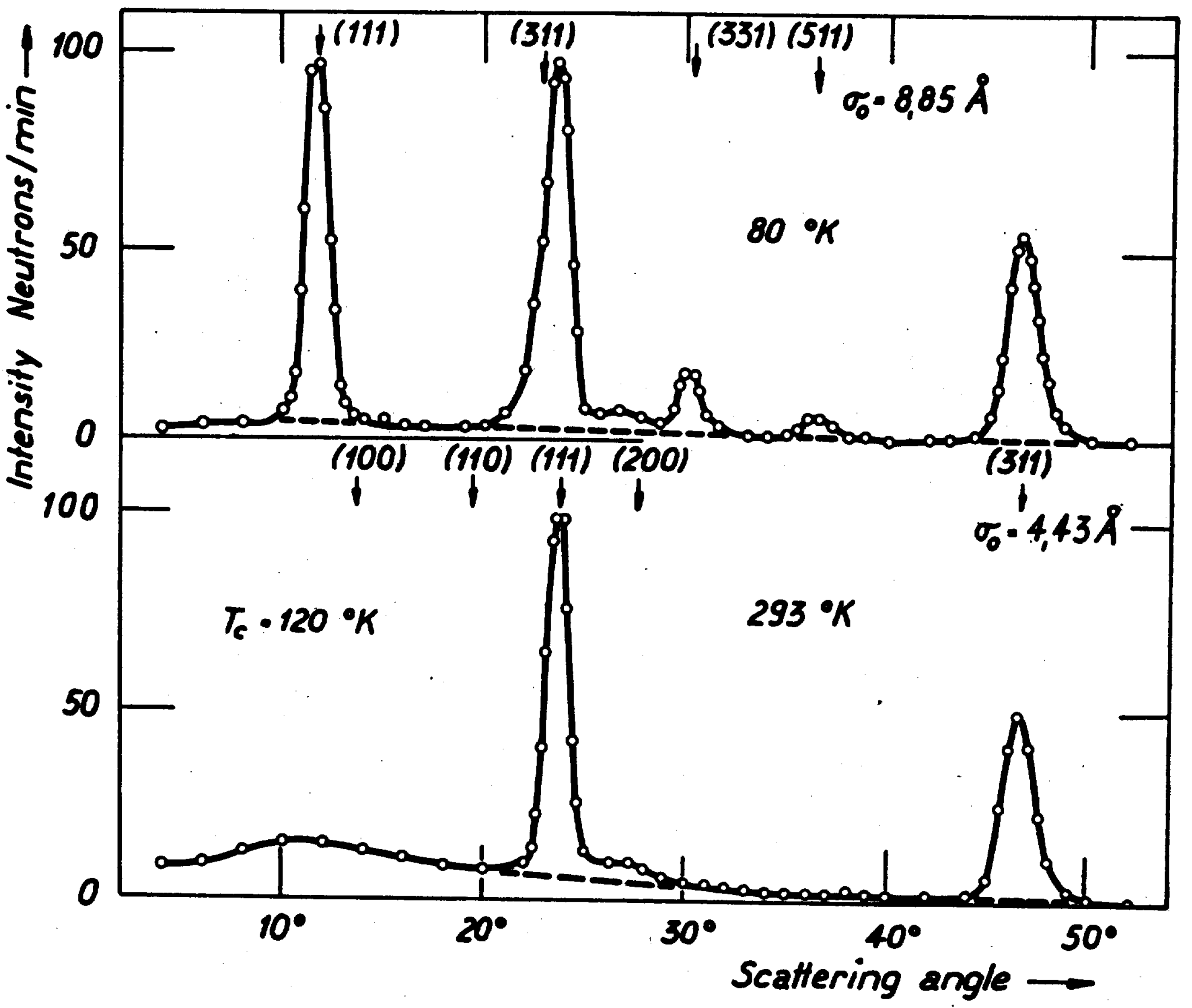

Fig. 13. Diffraction patterns for MnO taken below and above antiferromagnetic Néel temperature

and this results in coherent magnetic scattering of the neutron radiation. For these latter cases then, the coherent magnetic scattering will be superimposed upon the coherent nuclear scattering in the diffraction pattern and before interpretation of the pattern can be accomplished the two components must be separated.

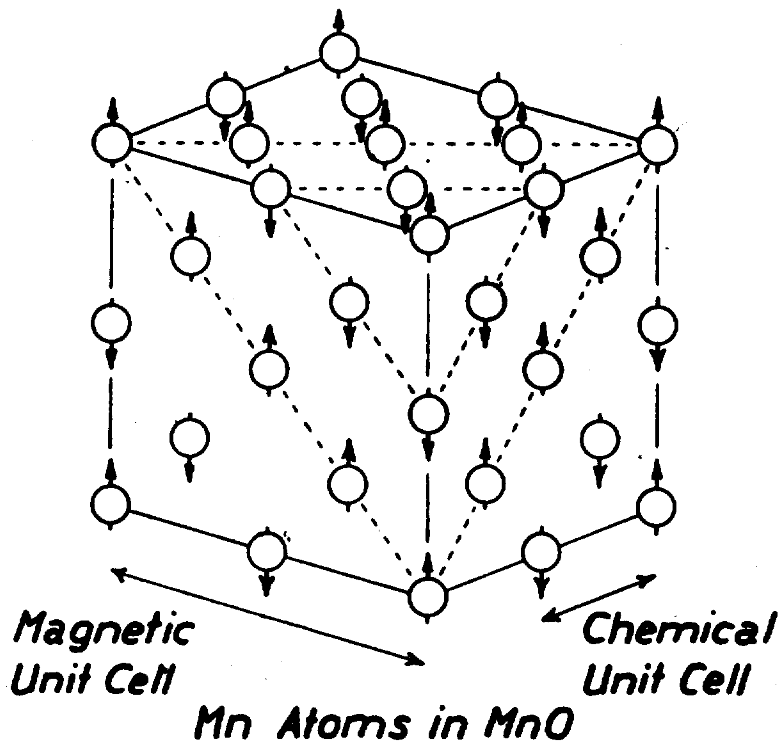

Fig. 14. Magnetic structure suggested in antiferromagnetic MnO (see text)

All of the magnetic scattering effects will be characterized by the form factor variation of differential scattering cross section in contrast to the isotropic nuclear scattering. This results because the electrons which are responsible for the atomic magnetic moment have a spatial distribution within the atom whose linear dimension is about the same as the neutron wavelength, i.e., one angstrom. It differs from the usual x-ray form factor because only a few of the many atomic electrons contribute to the atomic magnetic moment.

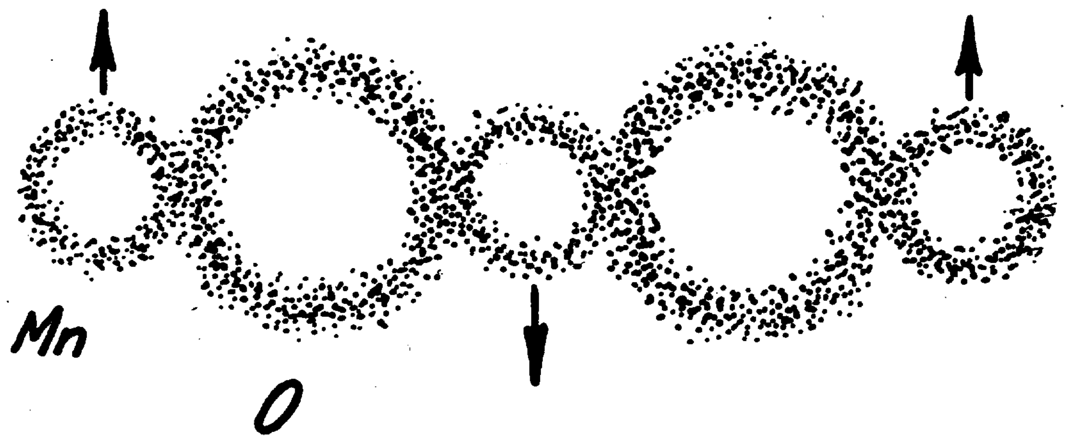

Fig. 15. Superexchange coupling in MnO

In fact by studying this magnetic form factor, much significant information can be obtained about the origin of the atomic magnetism.

One of the earliest magnetic substances to be investigated [5] was the oxide MnO which becomes antiferromagnetic at low temperatures with a Neel temperature of 120 °K. Fig. 13 shows powder diffraction patterns taken at 80° and 293 °K for this substance and one sees extra coherent scattering and considerably less diffuse scattering in the low temperature pattern. Thus the incoherent or diffuse scattering that characterizes the paramagnetic scattering is transformed into coherent, antiferromagnetic intensity when the atomic magnetic moments become locked into preferred orientations by the quantum mechanical exchange forces. It is to be noticed that the diffuse scattering in the higher temperature pattern shows a broad maximum in the forward direction of scattering and this is an indication of residual short range order in the magnetic structure. Additionally the coherent reflections at low temperature can not be indexed with the usual crystallographic unit cell ($a_0 = 4.43$ Å) but they can be indexed with a magnetic unit cell of twice the dimensions.

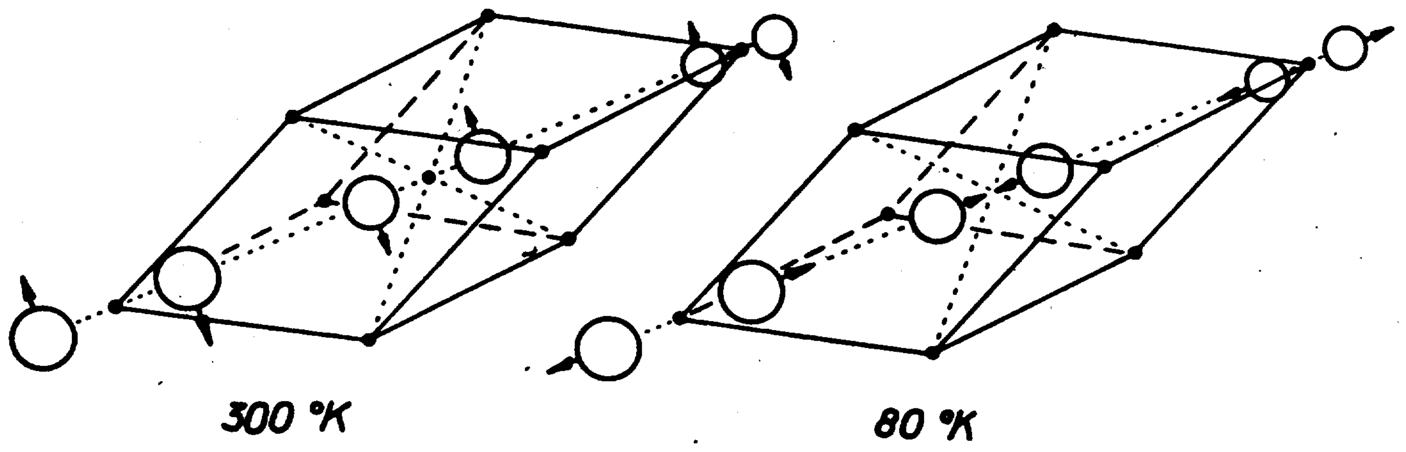

Fig. 16. Magnetic structure in antiferromagnetic alpha – Fe_2O_3

Fig. 14 shows the magnetic structure which is derived from the data and it is seen that the structure consists of (111) ferromagnetic sheets which alternate in positive and negative direction. From the relative intensities in the magnetic pattern it is sometimes possible to determine the direction of the magnetic axis relative to the crystallographic axes and for this substance the most recent unpublished data suggests this direction to be along the [111] axis rather than as shown in Fig. 14. Perhaps the most interesting feature of the magnetic structure is the antiparallel orientation of the next-nearest neighboring ions which is caused by the intervening oxygen ion. This phenomena, known as *superexchange* coupling of the magnetic moments, is illustrated in Fig. 15. Here the magnetic shell of the Mn atoms overlap electronic orbitals of an intervening oxygen ion and the direction of one moment is transmitted to another.

A second example of an antiferromagnetic lattice is shown in Fig. 16 as determined for α—Fe_2O_3 at two temperatures, 80 °K and 300 °K. At both temperatures there exist balanced pairs of magnetic mo-

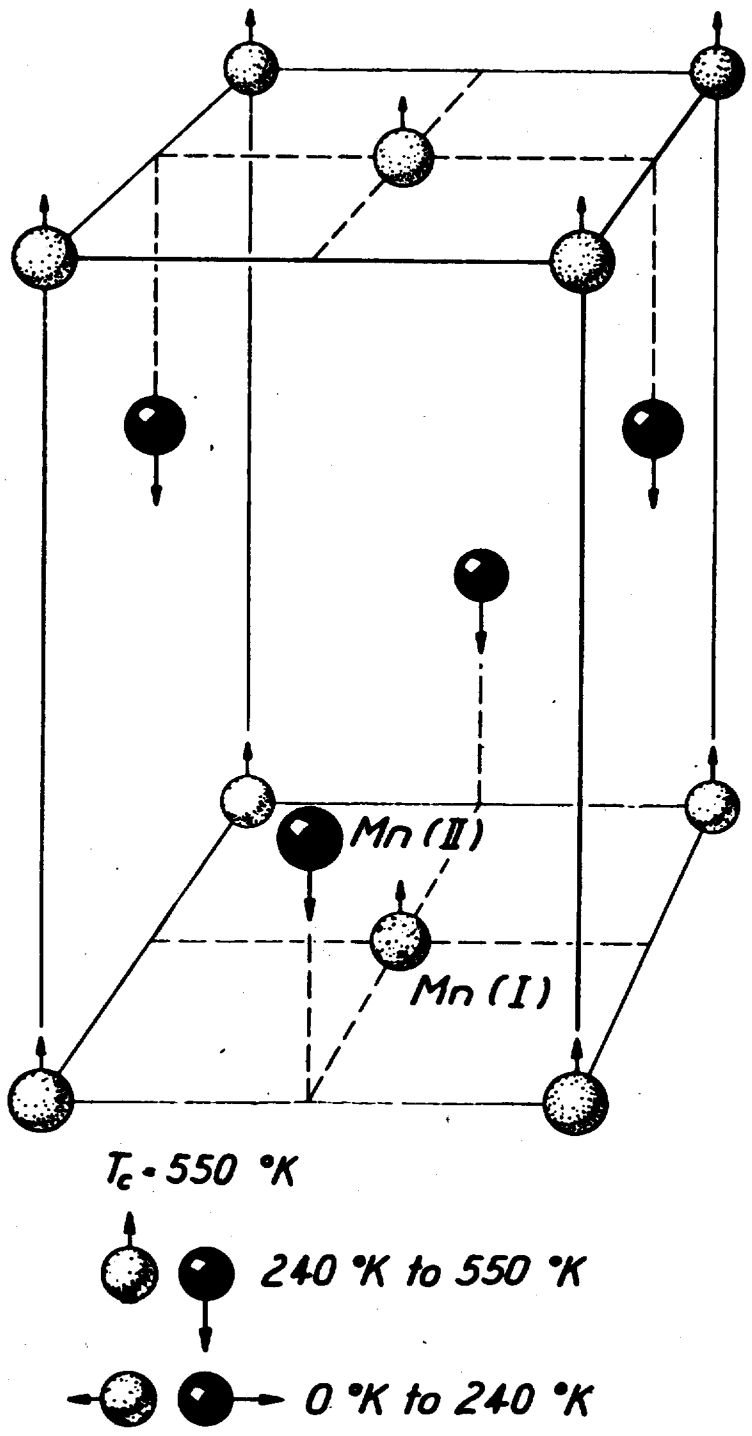

Fig. 17. Magnetic structure in Ferrimagnetic Mn_2Sb. The Mn (I) and Mn (II) ions differ in magnetic strength

ments but the direction of the magnetic axis differs at the two temperatures as shown. Again there exists an intervening layer of oxygen ions between antiferromagnetically coupled Fe ions.

Sometimes antiparallel coupling is found between ions of different magnetic strength and this type of substance is called *ferrimagnetic*. Many of the ferrite series of magnetic materials have been studied by neutron methods and established to be of this type. In illustration of this type of structure, Fig. 17 shows the magnetic structure which exists in Mn_2Sb. Two groups of Mn ions, Mn I and Mn II, are present in the substance and it has been established that these two ions possess magnetic moments of 2 and 4 *Bohr* magnetons respectively, with antiparallel orientation.

By procedures such as these, many magnetic structures have been studied as summarized in reference [1]. The details of the magnetic structure have demonstrated the mechanism of the electronic coupling that characterizes magnetic materials and offered considerable guidance in the development of the theory for such exchange coupling.

Literatur

[1] *G. E. Bacon*, Neutron Diffraction, Oxford University Press (1955). — *C. G. Shull* and *E. O. Wollan*, Solid State Physics — Vol. II, Academic Press (1956).
[2] *Rundle*, *Shull* and *Wollan*, Acta Cryst. **5**, 22 (1952).
[3] *G. E. Bacon* and *R. S. Pease*, Proc. Roy. Soc. **A 230**, 359 (1955).
[4] *G. Shirane*, *R. Pepinsky* and *B. C. Frazer*, Acta Cryt. **9**, 131 (1956).
[5] *Shull*, *Strauser* and *Wollan*, Phys. Rev. **83**, 333 (1951).